Electronic Supporting Information for:

Chiral supramolecular organization and cooperativity in DNA-templated assemblies of Zn^{II}-chromophore complexes

Jenifer Rubio-Magnieto,[a] Mohit Kumar,[b] Patrick Brocorens,[a] Julien Idé,[a]

Subi J. George,[b]* Roberto Lazzaroni,[a]* and Mathieu Surin[a]*

[a] *Laboratory for Chemistry of Novel Materials, Center for Innovation in Materials and Polymers, University of Mons - UMONS, 20 Place du Parc, B-7000 Mons, Belgium. E-mail: mathieu.surin@umons.ac.be; roberto.lazzaroni@umons.ac.be*

[b] *Supramolecular Chemistry Laboratory, New Chemistry Unit, Jawaharlal Nehru Centre for Advanced Scientific Research (JNCASR), Bangalore, India 560064. E-mail: george@jncasr.ac.in*

Table of contents:

Experimental Section

Synthesis and Characterization

PDPA and **NDPA** were synthesized based on the literature report.[1]

Sample preparation

All samples were prepared by injecting the stock solution of **PDPA** or **NDPA** into required volume of solvent (10 mM HEPES buffer). To that required amount of oligonucleotides were injected and the solution was mixed by manual shaking before measurements. The oligonucleotides (ODN) were purchased from Eurogentec (Belgium) with the highest purity grade (UltraPureGold™, RP - HPLC, > 95% pure in sequence,). The composition of the DNA was checked by MALDI-ToF. The oligonucleotides were also dissolved in a 10 mM HEPES buffer at a concentration of 100 μM (experimental estimation error for the stock concentration is around 7%). The concentration of DNA in the buffer solution was determined by UV-Vis absorption at 25 ºC using the specific extinction coefficients at 260 nm (ε_{260}) of each DNA, which are 243400 $L.mol^{-1}.cm^{-1}$ and 483400 $L.mol^{-1}.cm^{-1}$, for ssDNAd$(A)_{20}$ and ssDNAd$(A)_{40}$, respectively. The structure of these oligonucleotides is described in the main text. The experimental estimation error for a 10 μM concentration is around 10 %

UV-Vis absorption and Circular Dichroism spectroscopy

The UV-Vis absorption and CD measurements were recorded using a Chirascan™ Plus CD Spectrometer from Applied Photophysics. The measurements were carried out using 1 mm or 2 mm quartz suprasil cells from Hellma Analytics. The spectra were recorded between 240 and 650 nm, with a bandwidth of 1 nm, time per point 1 s and two repetitions. The CD RMS noise is around 0.04 mdeg at 500 nm. The buffered water solvent reference spectra were used as baselines and were automatically subtracted from the CD spectra of the samples.

Fluorescence spectroscopy

Emission spectra were recorded using a Perkin-Elmer LS55 spectrophotometer. Fluorescence measurements were carried out at 20 ºC by using a 10 mm quartz cells (1 mL) from Lightpath Optical. The excitation wavelength was set at 493 nm. The spectra were recorded between 520 and 900 nm, with 50 nm/min and slits = 15, 20. Minimum signal-to-noise level using the Raman band of water, excitation 350 nm, is 750:1 RMS measuring noise on the Raman peak, and 2500:1 RMS measuring noise on the baseline

Molecular Modelling Methodology

A left-handed stack of 20 **PDPA** molecules linked to two single-stranded $\mathbf{dA_{20}}$ has been modeled with the Materials Studio 6.0 modeling package (Biovia, formerly Accelrys), by molecular mechanics (MM) and molecular dynamics (MD) methods. A modified Dreiding[2] force field was used, as described previously[3]. A chloride anion was added per Zn atom to maintain the neutrality of the system. The initial distance between the planes of adjacent PDPA in the stacks was initially 3.7 Å and the angle between the neighbouring molecules was set to 45° to avoid steric crowding. The assembly was optimized by a MM, then was submitted to a 2 ns relaxation MD with the chloride ions linked to the zinc atoms, to relax most of the steric constraints in the assembly. Then, the chloride ions were left free to move, a short MM was again performed, followed by a MD run of 2 ns. The analyses (CD spectra, structure characterization) were performed on the second part of the MD trajectory. The MM energy minimizations were performed with a conjugate gradient algorithm until a convergence criterion of 0.001 kcal/mol.Å or 500 iterations was reached. The long-range interaction cutoff distance was set to 14 Å with a spline width of 3 Å. The charges on the atoms were assigned from the PCFF force field.[4,5] The MD simulations were performed in the canonical (N,V,T) ensemble. The Nosé thermal bath coupling[6] was used to maintain the temperature at 300 K, with a coupling constant of 0.05. The Verlet velocity algorithm was used to integrate the equations of motion with a 1 fs time step.

To account for thermal fluctuations, the absorption and CD spectra of the PDPA assemblies were calculated and averaged over the second part of the MD. Since we are interested in the optical response of the chromophore, we removed the DNA strand, the Zn atoms and the chloride anions from the system in order to reduce the computational effort and we applied the excitonic model to

each frame: A supra-molecular Hamiltonian was built on the basis of localised excited states. Those states were obtained from CIS calculations performed on individual molecules using the ZINDO parameterization implemented in the Gaussian package[7]. To ensure the convergence of the spectra at high energy, 100 excited states have been considered. After diagonalization of this Hamiltonian, supra-molecular transition dipole and magnetic moments were calculated and used to compute the oscillator and rotatory strengths. Finally, a Gaussian broadening of 0.2 eV was applied before averaging over the MD. Note that this approach does not account for the vibronic structure observed in the experimental spectra.

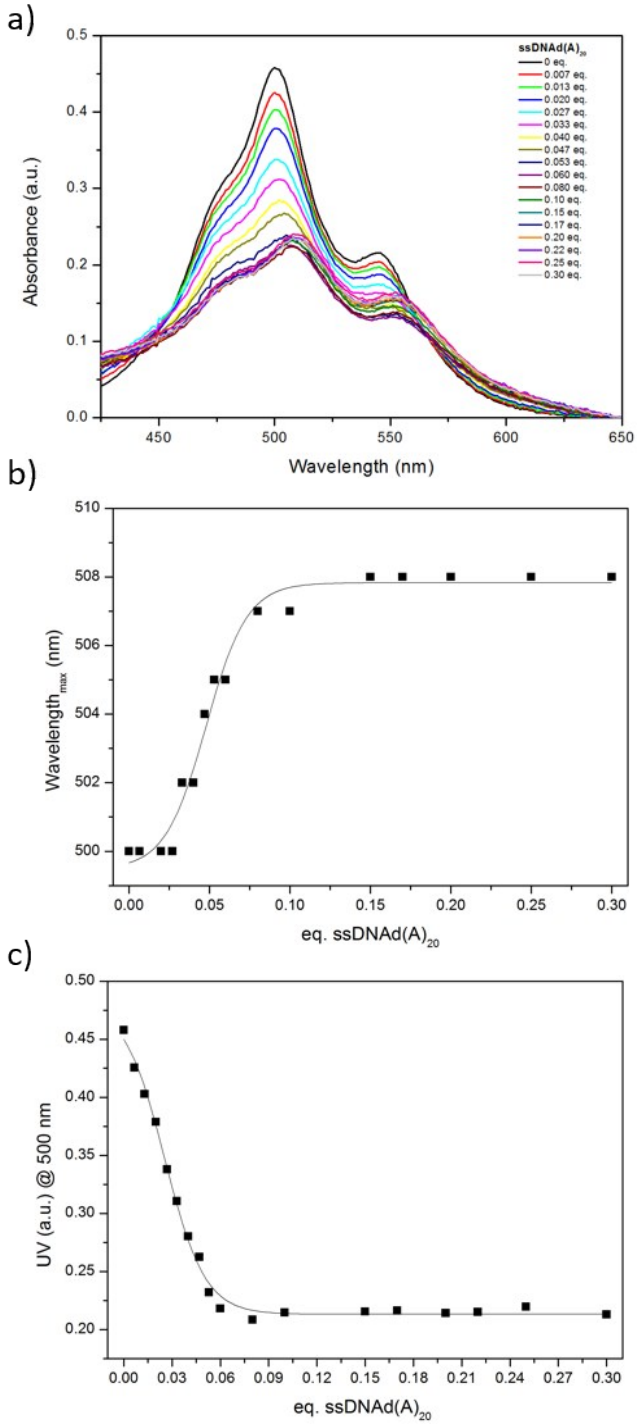

Figure S1. Binding of ssDNAd$(A)_{20}$ to PDPA-assembly: a) Variation in UV-Vis spectra of PDPA (aq. HEPES solution, c = 50 μM) upon titration with ssDNAd$(A)_{20}$. Legends in the graph represent molar equivalents with respect to PDPA; b) Variation in λ_{max} plotted against mole fraction, and c) plot of UV-Vis intensity at 500 nm upon ssDNA titration represented in mole fraction.

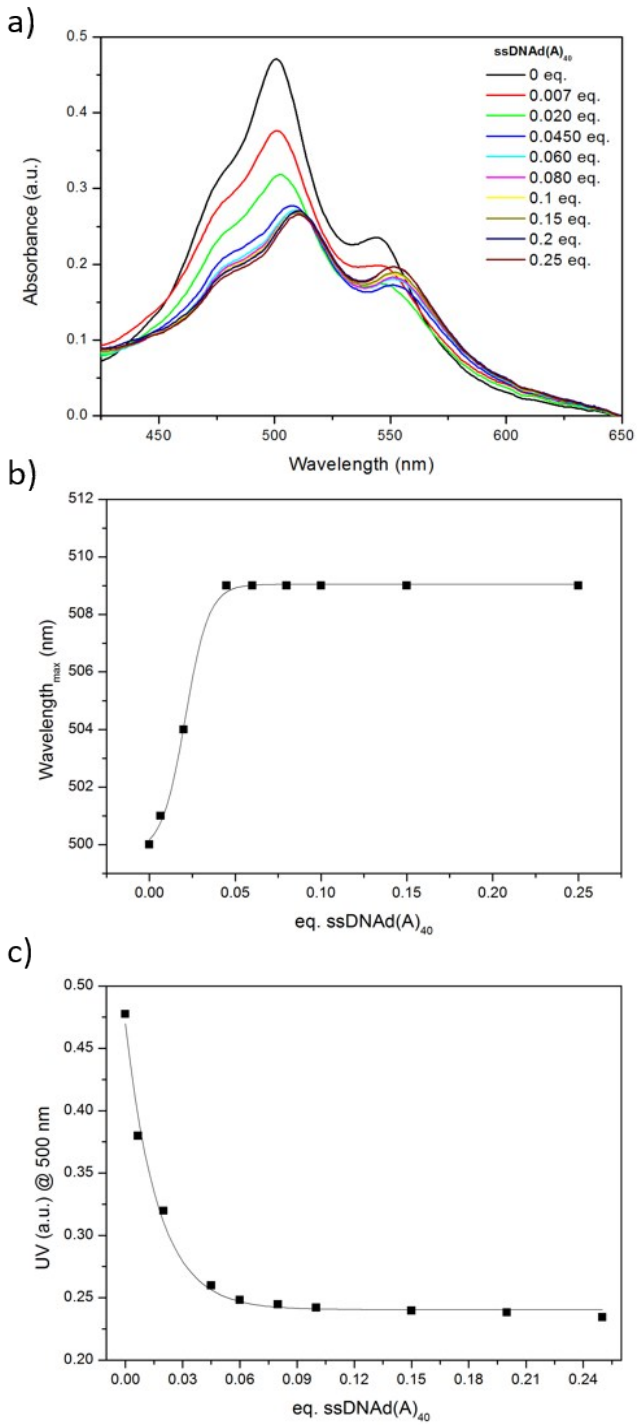

Figure S2. Binding of ssDNAd$(A)_{40}$ to PDPA-assembly: a) Variation in UV-Vis spectra of PDPA (aq. HEPES solution, c = 50 µM) upon titration with ssDNAd$(A)_{40}$. Legends in the graph represent molar equivalents with respect to PDPA; b) Variation in λ_{max} plotted against mole fraction, and c) plot of UV-Vis intensity at 500 nm upon ssDNA titration represented in mole fraction.

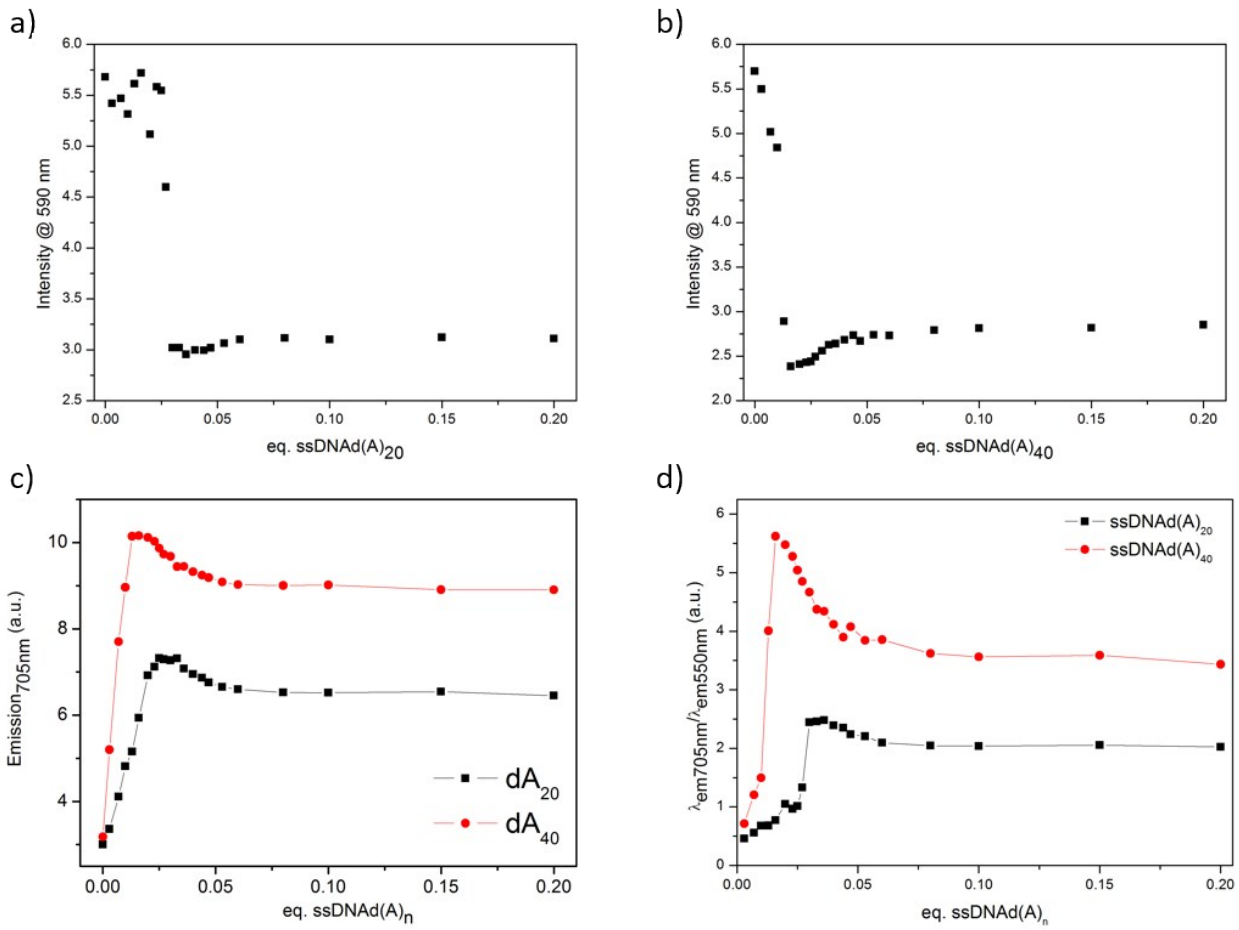

Figure S3. Emission spectral changes of PDPA assembly, induced by DNA: Plot of Emission intensity at 590 nm upon ssDNA titration for a) ssDNAd$(A)_{20}$ and b) ssDNAd$(A)_{40}$. c) Plot of the lambda emission at 705 nm upon ssDNA titration for ssDNAd$(A)_{20}$ and ssDNAd$(A)_{40}$. d) Plot of the lambda emission at 705 nm/550 nm upon ssDNA titration for ssDNAd$(A)_{20}$ and ssDNAd$(A)_{40}$. All measurements were done in aq. HEPES solution, c = 5 µM PDPA, and with λ_{exc} = 493 nm.

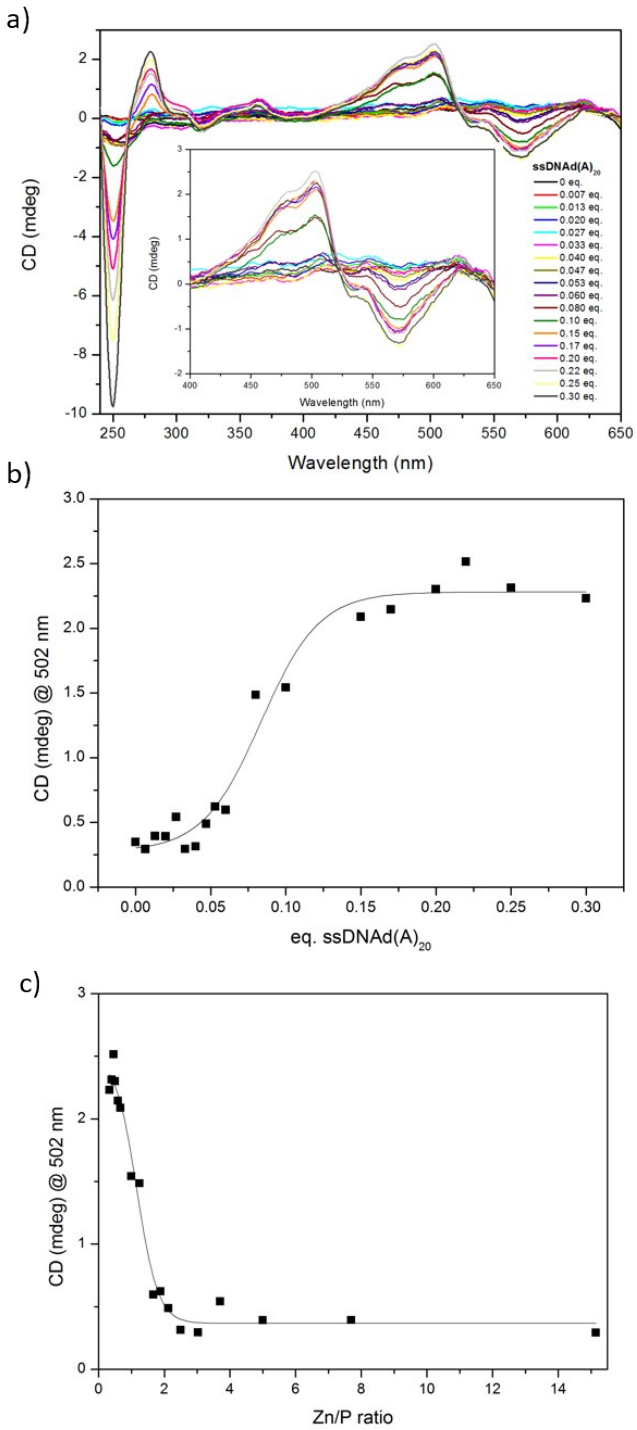

Figure S4. Binding of ssDNAd$(A)_{20}$ to PDPA-assembly: a) Variation in CD spectra of PDPA (aq. HEPES solution, c = 50 μM) upon titration with ssDNAd$(A)_{20}$. Legends in the graph represent molar equivalents with respect to PDPA. Plot of CD intensity monitored at 502 nm against b) mole fraction and c) Zn/P ratio (number of Zn^{II} carried out by PDPA system (Zn) with respect to the number of phosphate groups present on ssDNA (P)).

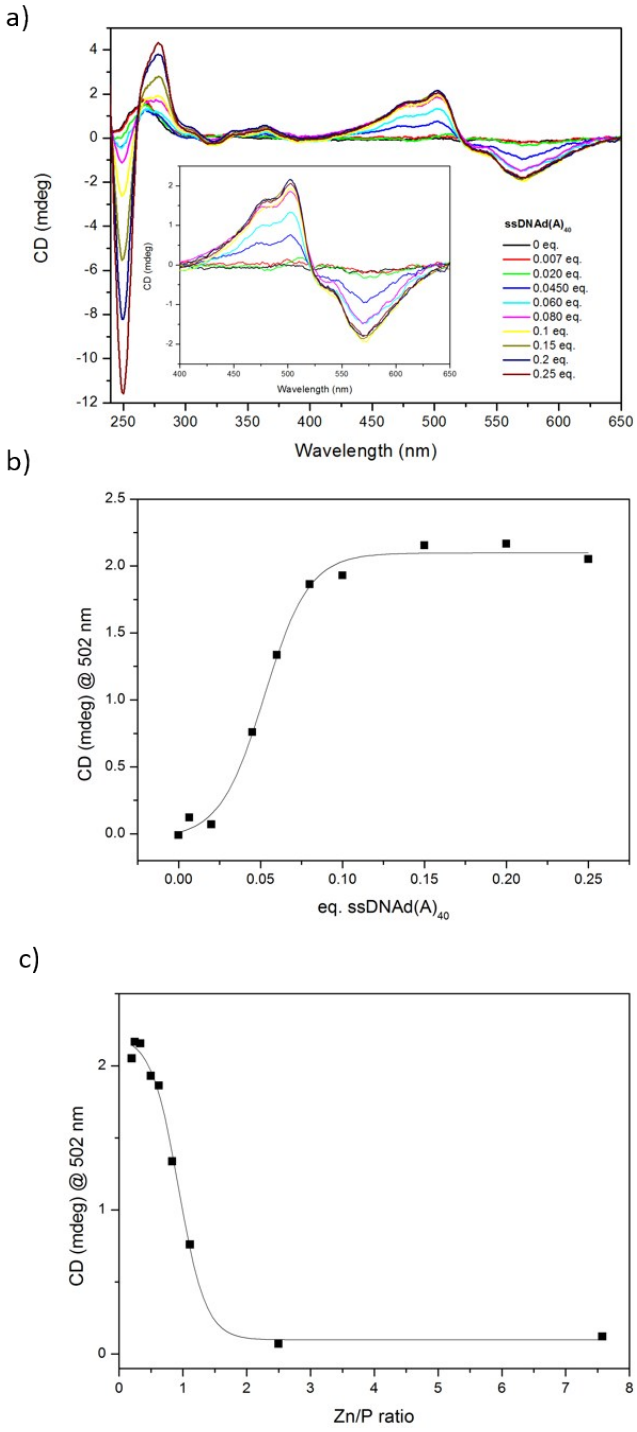

Figure S5. Binding of ssDNAd$(A)_{40}$ to PDPA-assembly: a) Variation in CD spectra of PDPA (aq. HEPES solution, c = 50 μM) upon titration with ssDNAd$(A)_{40}$. Legends in the graph represent molar equivalents with respect to PDPA. Plot of CD intensity monitored at 502 nm against b) mole fraction and c) Zn/P ratio (number of Zn^{II} carried out by PDPA system (Zn) with respect to the number of phosphate groups present on ssDNA (P)).

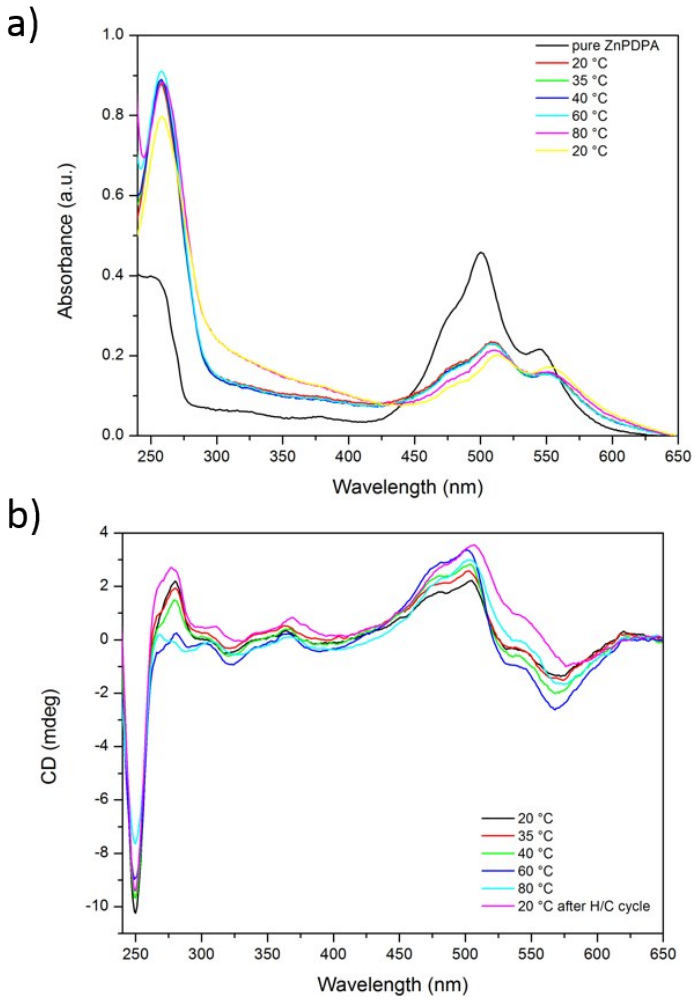

Figure S6. Binding of ssDNAd$(A)_{20}$ to PDPA-assembly: Variation in a) UV-Vis and b) CD spectra of PDPA(aq. HEPES solution, c = 50 µM):ssDNAd$(A)_{20}$ 1:0.3 upon temperature increase from 20 ºC to 80 ºC and after a heating/cooling cycle (pink line).

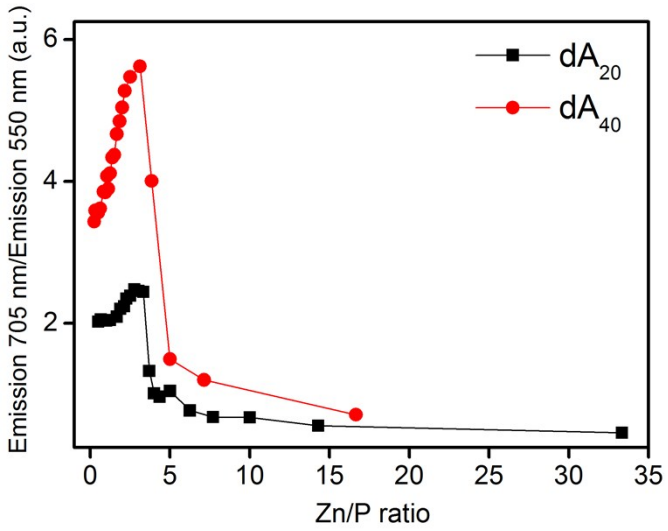

Figure S7. Ratio between emission intensities of PDPA at 705 nm (excimer) to 550 nm upon the addition of DNA template dA_n (buffered aqueous solution), shown as a function of the number on Zn atoms per phosphate group of the oligonucleotide.

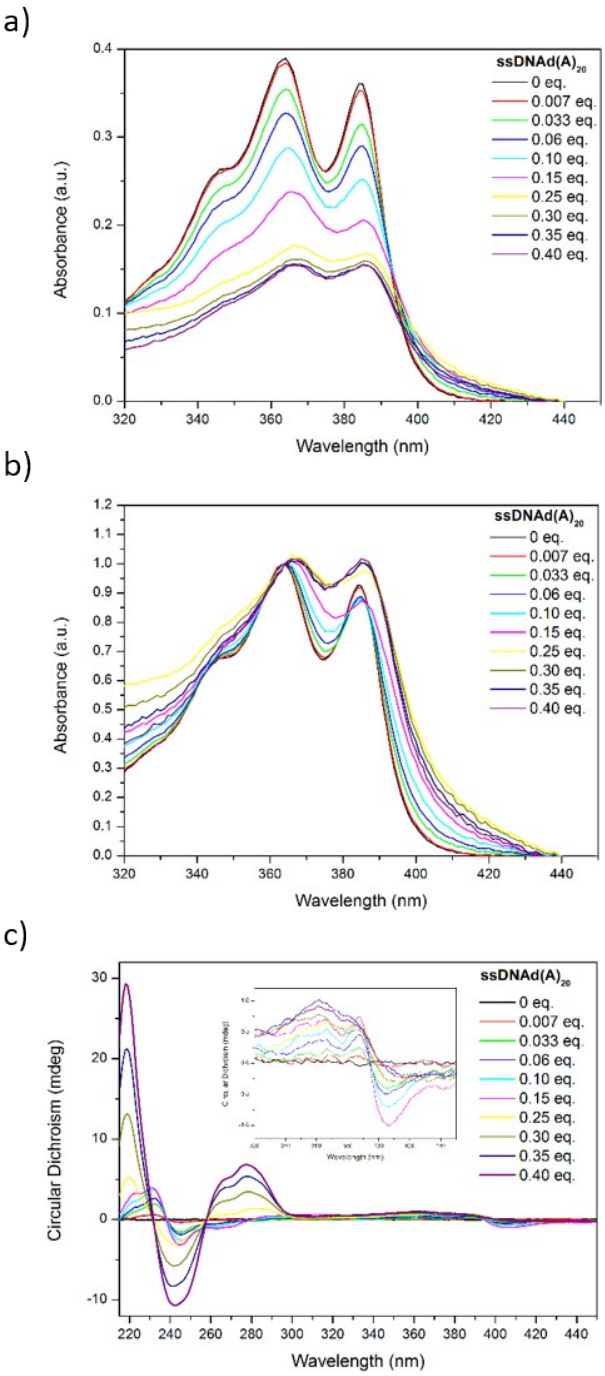

Figure S8. Binding of ssDNAd$(A)_{20}$ to NDPA-assembly: Variation in UV-Vis (a) and Normalized UV-Vis (b) spectra of NDPA, and in CD (c) (aq. HEPES solution, c = 50 μM) upon titration with ssDNAd$(A)_{20}$. Legends in the graph represent molar equivalents with respect to NDPA.

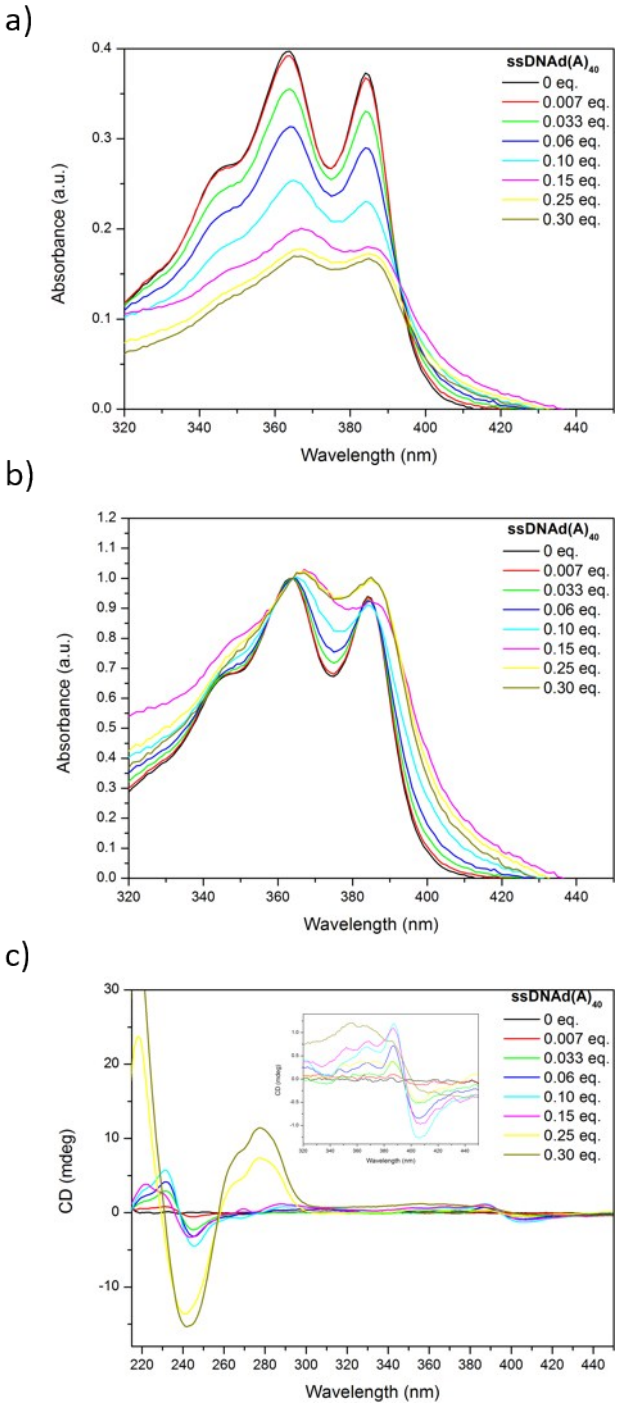

Figure S9. Binding of ssDNAd$(A)_{40}$ to NDPA-assembly: Variation in UV-Vis (a) and Normalized UV-Vis (b) spectra of NDPA, and in CD (c) (aq. HEPES solution, c = 50 μM) upon titration with ssDNAd$(A)_{40}$. Legends in the graph represent molar equivalents with respect to NDPA.

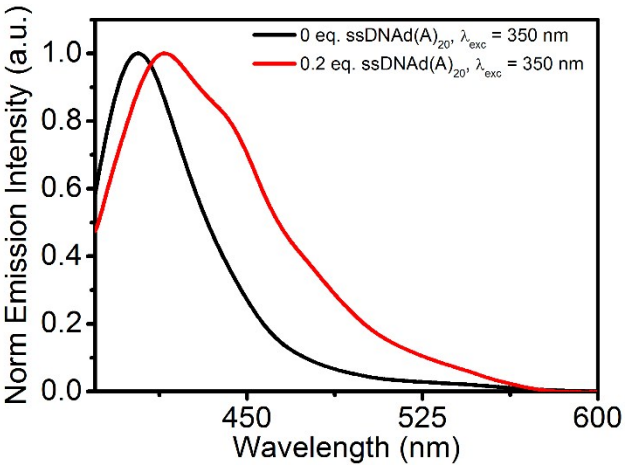

Figure S10. Emission spectral changes of NDPA assembly, induced by DNA: Normalized Emission intensity upon ssDNAd$(A)_{20}$ adition. All measurements were done in aq. HEPES solution, c = 5 μM NDPA, and with λ_{exc} = 350 nm.

References

1 H. N. Lee, Z. Xu, S. K. Kim, K. M. K. Swamy, Y. Kim, S.-J. Kim and J. Yoon, *J. Am. Chem. Soc.*, 2007, **129**, 3828; X. Chen, M. J. Jou and J. Yoon, *Org. Lett.*, 2009, **11**, 2181.

2 S. L. Mayo, B. D. Olafson; W. A. Goddard III, *J. Phys. Chem.* 1990, **94**, 8897-8909.

3 M. Kumar, P. Brocorens, C. Tonnelé, D. Beljonne, M. Surin and S. J. George, *Nat. Commun.*, 2014, **5**, 5793.

4 H. Sun, *J. Comput. Chem.* 1994, **15**, 752-768 Sun, H. Ab initio calculations and force field development for computer simulation of polysilanes. *Macromolecules* **28**, 701-712 (1995).

5 H. Sun, *Macromolecules* 1995, **28**, 701-712.

6 S. A. Nosé, *Mol. Phys,* 1984, **52**, 255-268.

7 Gaussian 09, Revision E.01, M. J. Frisch, G. W. Trucks, H. B. Schlegel, G. E. Scuseria, M. A. Robb, J. R. Cheeseman, G. Scalmani, V. Barone, B. Mennucci, G. A. Petersson, H. Nakatsuji, M. Caricato, X. Li, H. P. Hratchian, A. F. Izmaylov, J. Bloino, G. Zheng, J. L. Sonnenberg, M. Hada, M. Ehara, K. Toyota, R. Fukuda, J. Hasegawa, M. Ishida, T. Nakajima, Y. Honda, O. Kitao, H. Nakai, T. Vreven, J. A. Montgomery, Jr., J. E. Peralta, F. Ogliaro, M. Bearpark, J. J. Heyd, E. Brothers, K. N. Kudin, V. N. Staroverov, R. Kobayashi, J. Normand, K. Raghavachari, A. Rendell, J. C. Burant, S. S. Iyengar, J. Tomasi, M. Cossi, N. Rega, J. M. Millam, M. Klene, J. E. Knox, J. B. Cross, V. Bakken, C. Adamo, J. Jaramillo, R. Gomperts, R. E. Stratmann, O. Yazyev, A. J. Austin, R. Cammi, C. Pomelli, J. W. Ochterski, R. L. Martin, K. Morokuma, V. G. Zakrzewski, G. A. Voth, P. Salvador, J. J. Dannenberg, S. Dapprich, A. D. Daniels, Ö. Farkas, J. B. Foresman, J. V. Ortiz, J. Cioslowski, and D. J. Fox, Gaussian, Inc., Wallingford CT, 2009.